ISSN 1063-7737, Astronomy Letters, 2016, Vol. 42, No. 12, pp. 815–824. © Pleiades Publishing, Inc., 2016.
Original Russian Text © V.G. Klochkova, V.E. Panchuk, N.S. Tavolzhanskaya, 2016, published in Pis'ma v Astronomicheskii Zhurnal, 2016, Vol. 42, No. 12, pp. 897–907.

New in the Optical Spectrum and Kinematic State of the Atmosphere of the Variable V1027 Cyg (=IRAS 20004+2955)

V. G. Klochkova*, V. E. Panchuk, and N. S. Tavolzhanskaya

Special Astrophysical Observatory, Russian Academy of Sciences, Nizhnii Arkhyz, Karachai-Cherkessian Republic, 369167 Russia

Received June 23, 2016

Abstract—Based on our high-spectral-resolution observations performed with the NES echelle spectrograph of the 6-m telescope, we have studied the peculiarities of the spectrum and the velocity field in the atmosphere and envelope of the cool supergiant V1027 Cyg, the optical counterpart of the infrared source IRAS 20004+2955. A splitting of the cores of strong absorptions of metals and their ions (Si II, Ni I, Ti I, Ti II, Sc II, Cr I, Fe I, Fe II, BaII) has been detected in the stellar spectrum for the first time. The broad profile of these lines contains a stable weak emission in the core whose position may be considered as the systematic velocity $V_{\rm sys} = 5.5$ km s^{-1}. Small radial velocity variations with an amplitude of 5–6 km s^{-1} due to pulsations have been revealed by symmetric low- and moderate-intensity absorptions. A long-wavelength shift of the Hα profile due to line core distortion is observed in the stellar spectrum. Numerous weak CN molecular lines and the KI 7696 Å line with a P Cyg profile have been identified in the red spectral region. The coincidence of the radial velocities measured from symmetric metal absorptions and CN lines suggests that the CN spectrum is formed in the stellar atmosphere. We have identified numerous diffuse interstellar bands (DIBs) whose positions in the spectrum, V_r(DIBs) = -12.0 km s^{-1}, correspond to the velocity of the interstellar medium in the Local Arm of the Galaxy.

DOI: 10.1134/S1063773716120033

Keywords: *stars, evolution, AGB stars, circumstellar envelopes, spectra.*

INTRODUCTION

The cool supergiant V1027 Cyg of MK spectral type Sp = G7 Ia (Keenan and McNeil 1989) is identified with the infrared (IR) source IRAS 20004+2955. Volk and Kwok (1989) modeled the peculiar, very flat, IR spectrum of IRAS 20004+2955 and concluded that the object is observed at the very beginning of the evolutionary transition from the asymptotic giant branch (AGB) to a planetary nebula. Kwok (1993) entered this star in his widely known list of protoplanetary nebula (PPN) candidates, stars in transition to the planetary nebular stage. However, V1027 Cyg has remained poorly studied until the present time; there is no consensus on the evolutionary status of this star.

Based on UBV photometry and low-resolution spectroscopy, Arkhipova et al. (1992) classified this star as a semiregular variable with an amplitude of brightness variations increasing from V to U from 0.4 to 0.8 mag. These authors concluded that interstellar extinction is responsible for the bulk of the reddening in V1027 Cyg, while the pattern of brightness and color variability suggested that its variability is caused by pulsations. Subsequently, having measured the radial velocities V_r with a correlation spectrometer, Arkhipova et al. (1997) detected a radial velocity variability in the range from -10 to $+20$ km s^{-1} and pointed out a strengthening of BaII lines. All the values of V_r from Hrivnak and Wenxian (2000) also fit into this velocity range.

Based on the spectra taken with the echelle spectrograph of the 6-m telescope, Klochkova et al. (2000a) determined the main parameters of V1027 Cyg (effective temperature $T_{\rm eff} = 5000$ K, surface gravity $\log g = 1.0$), its metallicity $[{\rm Fe/H}]_\odot = -0.2$, and the abundances of 16 elements in the stellar atmosphere by the model atmosphere method. The nearly solar metallicity in combination with the low radial velocity of the star suggest that V1027 Cyg belongs to the Galactic disk population. Taranova et al. (2009) performed long-term $JHKLM$ photometry for yellow supergiants and detected a small-amplitude ($\leq 0.25^m$) IR brightness variability with a probable period of about 237 days in V1027 Cyg. Using the same observations, Bogdanov and Taranova (2009) computed the model of a spherical

*E-mail: valenta@sao.ru

Table 1. Times of observations of V1027 Cyg with the NES spectrograph of the 6-m telescope and the recorded wavelength range $\Delta\lambda$ in Å. The heliocentric radial velocities V_r measured from symmetric absorptions (abs.), Hα cores, and DIBs are given. The number of lines used to determine V_r is given in parentheses

Date	JD−2450000	$\Delta\lambda$, Å	V_r, km s^{-1}		
			abs.	Hα	DIBs
Oct. 13, 2013	6579.32	4000–6980	-4.1 ± 0.1 (332)	+11.9	-11.4 ± 0.4 (15)
Apr. 28, 2015	7141.14	5400–8470	$+4.5 \pm 0.1$ (264)	+13.3	-12.9 ± 0.5 (13)
			$+4.0 \pm 0.3$ (24, CN)		
Sep. 3, 2015	7269.36	4000–6980	$+9.1 \pm 0.1$ (541)	+7.9	-11.7 ± 0.4 (10)

circumstellar envelope and estimated the mass loss rate to be $1.3 \times 10^{-5} M_\odot$ yr^{-1}.

The radial velocity variability of V1027 Cyg and the evidence for the peculiarity of its spectrum found by Klochkova et al. (2000a) serve to us as a stimulus to continue the observations of V1027 Cyg. In this paper we present the results of our optical spectroscopy for this star performed with the 6-m telescope over several nights in 2013–2015. The goal of these observations is a detailed study of the stellar spectrum and its possible variability as well as the kinematic state of the atmosphere of V1027 Cyg, its circumstellar envelope, and the interstellar medium toward this star with Galactic coordinates $l = 67.4°$ and $b = -0.3°$.

Our observational data are briefly described in the next section. Subsequently, we provide information about the peculiarities of the profiles for the spectral features detected from high-resolution spectra, analyze them, and discuss our results. Our brief conclusions are presented in the last section.

OBSERVATIONAL DATA

We took the spectra of V1027 Cyg at the Nasmyth focus of the 6-m telescope with the NES echelle spectrograph (Panchuk et al. 2007, 2009). In combination with an image slicer (Panchuk et al. 2003), the NES spectrograph provides a spectral resolution $R \approx 60\,000$ in a wide wavelength range. A 2048×4096-pixel CCD array has been used at the NES spectrograph since 2011, which has allowed the simultaneously recorded spectral range to be extended considerably. The times of observations of V1027 Cyg with the 6-m telescope and the recorded spectral range are given in Table 1.

In addition, for comparison, we invoke the stellar spectra taken during several observational sets in 1997 with the NES and PFES echelle spectrographs and used in Klochkova et al. (2000a). The NES spectrograph in its first modification in combination with a $1k \times 1k$ CCD array provided a resolution $R \approx 35\,000$. The PFES spectrograph designed for the observations of faint stars with a resolution $R \approx 15\,000$ (Panchuk et al. 1997) is mounted at the prime focus of the 6-m telescope.

The details of our spectrophotometric and positional measurements in the spectra were described in previously published papers; the corresponding references to them were given by Klochkova (2014). Note that applying the image slicer required a significant modification of the standard ECHELLE procedures of the MIDAS software package. The cosmic-ray particle hits were removed by median averaging of two spectra taken successively one after another. The wavelength calibration was performed using the spectra of a hollow-cathode Th–Ar lamp. The data were extracted from two-dimensional echelle spectra with the software package described in Yushkin and Klochkova (2005). The latest version of the DECH code (Galazutdinova 1992) was used to reduce the extracted spectra. In particular, it allows the radial velocities to be measured from individual features of complex lines typical of the spectra of the investigated stars. The positional zero point of each spectrogram was determined in a standard way, by referencing to the positions of ionospheric night-sky emission features and telluric absorption lines, which are observed against the background of the object's spectrum. The accuracy of measuring the velocity from one line in the NES spectra is $\sim$1.0 km s^{-1}.

MAIN RESULTS

Previously Unknown Peculiarities of the Spectrum

On the whole, the high-resolution optical spectrum of V1027 Cyg corresponds to its MK classification G7 Ia (Keenan and McNeil 1989). The absence of a visible emission in Hα is quite unexpected for a pulsating variable (see Fig. 1). An emission in Hα was also absent in the earlier spectra of this star taken with the 6-m telescope and used by Klochkova et al. (2000a) to determine the atmospheric chemical composition of this star. A strong (above the continuum level) and time-variable emission is a typical

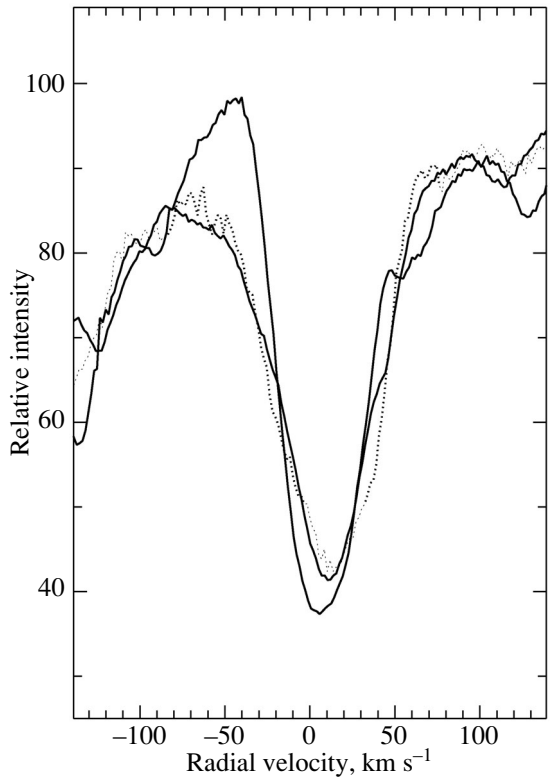

Fig. 1. Hα profiles in the spectrum of V1027 Cyg for three dates of observations: October 13, 2013 (thick solid curve), April 28, 2015 (dotted curve), and September 3, 2015 (thin solid curve).

signature of long-period variables (LPVs). The well-studied LPV star R Sct, in the optical spectra of which the intensity of the emission in Hα at some phases exceeds the continuum level manyfold (Lèbre and Gillet 1991; Kipper and Klochkova 2013), can serve as an example. An equally powerful emission in Hα was recorded by Klochkova et al. (2006) in the spectrum of the AGB star identified with the IR source IRAS 20508+2011. Over the four-year period of observations of this star with the 6-m telescope the absorption–emission Hα profile changed from a bell-shaped emission with a weak absorption in the core to a double-peaked emission with a central absorption lying below the continuum.

However, in the absence of an emission in Hα, we detected a number of other, subtler peculiarities in the spectrum of V1027 Cyg due to the high quality of our observational data. We saw a new peculiarity of strong absorptions: the lines with a low lower-level excitation potential ($\chi_{\rm low} < 1.5$ eV) have a complex profile including two absorptions with close intensities separated by an emission peak. To illustrate this peculiarity, Fig. 2 presents a fragment of the spectrum containing the strong and split Mg I, Fe I, Fe II, and Ti II absorptions. In addition, it emerged that the profiles of such strong absorptions are variable in time. In Fig. 3, where the profiles of the two strong Ba II 6141 Å and Fe I 6393 Å absorptions in the spectra taken on different dates are compared, apart from line doubling, line depth variability is clearly seen. The difference in the behavior of lines with different intensities is shown in Fig. 4, where the profiles of the medium-intensity Fe II 6147 Å line are compared with the Ba II 6141 Å line profiles.

As can be seen from Figs. 3 and 4, the blue wing in the short-wavelength component of the Ba II 6141 line is steeper than the red wing of the long-wavelength component. This difference may point to a difference between the physical conditions under which these spectral features are formed. The shape of the long-wavelength absorption profile is more stable, while the shape of the blue wing in the short-wavelength absorption changes significantly with time. The blue wing of the strong absorptions can be assumed to be formed under unstable conditions in the outer layers of the supergiant's extended atmosphere affected by pulsations. Note also that the blue wing in the short-wavelength absorptions changes synchronously with the Hα core.

It is important to emphasize in connection with the revealed anomalies of the strong absorptions that the abundances of chemical elements in the atmosphere of V1027 Cyg calculated previously by Klochkova et al. (2000a) do not require any correction, because in their calculations these authors used lines of a limited intensity with equivalent widths smaller than 200 mÅ.

The only emission whose intensity exceeds considerably the continuum level in the spectrum of V1027 Cyg is the emission component of the K I 7696 Å line. The P Cyg profile of this line in "relative intensity–radial velocity" coordinates is presented in Fig. 5 in comparison with the profile of the resonance Na I D lines. Comparison of the K I 7696 Å and Na I D line profiles allows us to suspect the presence of a weak emission feature in the long-wavelength wing of the Na I D lines.

Kinematic State of the Stellar Atmosphere

The presence of peculiarities in the profiles of strong lines and their variability suggest that differential line shifts are probable in the spectrum and that these shifts are variable in time. Therefore, for our search of radial velocity variations we selected low- and moderate-intensity absorptions with symmetric profiles without any visible peculiarities. Such absorptions are formed in deep layers of the stellar atmosphere and are not subjected to the possible influence of kinematic effects in the uppermost layers of the extended atmosphere. Tables 1 and 2 present the heliocentric radial velocities V_r measured from

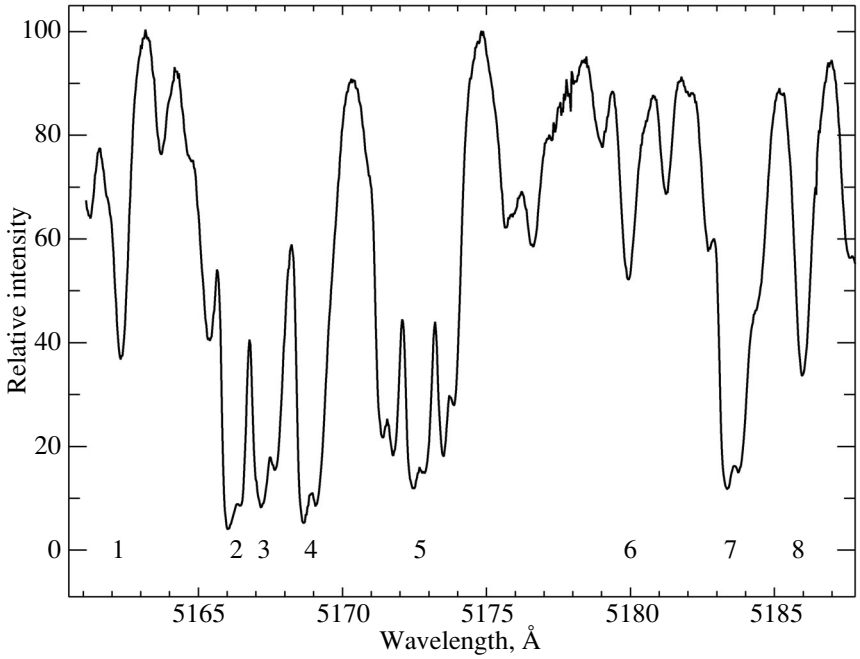

Fig. 2. Fragment of the September 3, 2015 spectrum for V1027 Cyg in the spectral region saturated by absorptions with split cores. The identified main absorptions are indicated: Fe I 5162.3 Å (1), Fe I 5166.3 Å (2), Mg I 5167.3 Å (3), Fe II 5169.0 Å (4), Mg I 5172.7 Å (5), Fe I 5180.1 Å (6), Mg I 5183.6 Å (7), and Ti II 5185.9 Å (8).

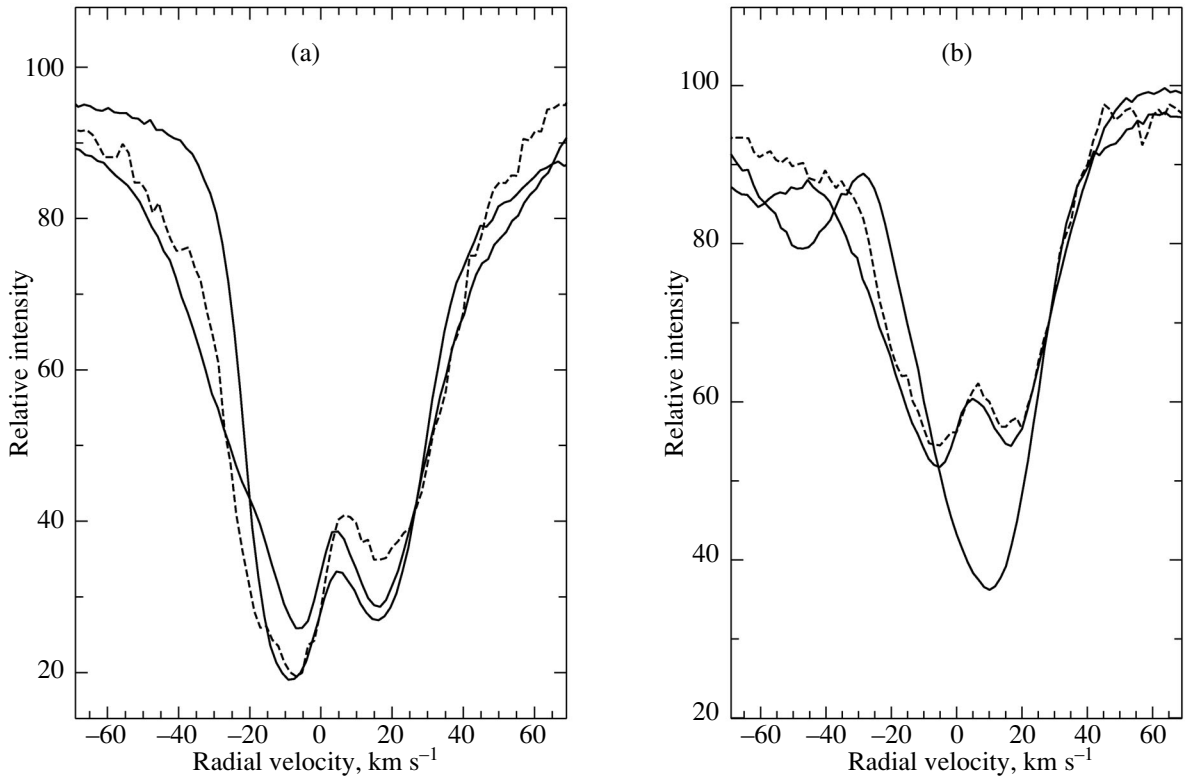

Fig. 3. Split Ba II 6141.42 Å (a) and Fe I 6393.6 Å (b) line profiles in the spectra of V1027 Cyg for three dates of observations: October 13, 2013 (thick solid curve), April 28, 2015 (dashed curve), and September 3, 2015 (thin solid curve).

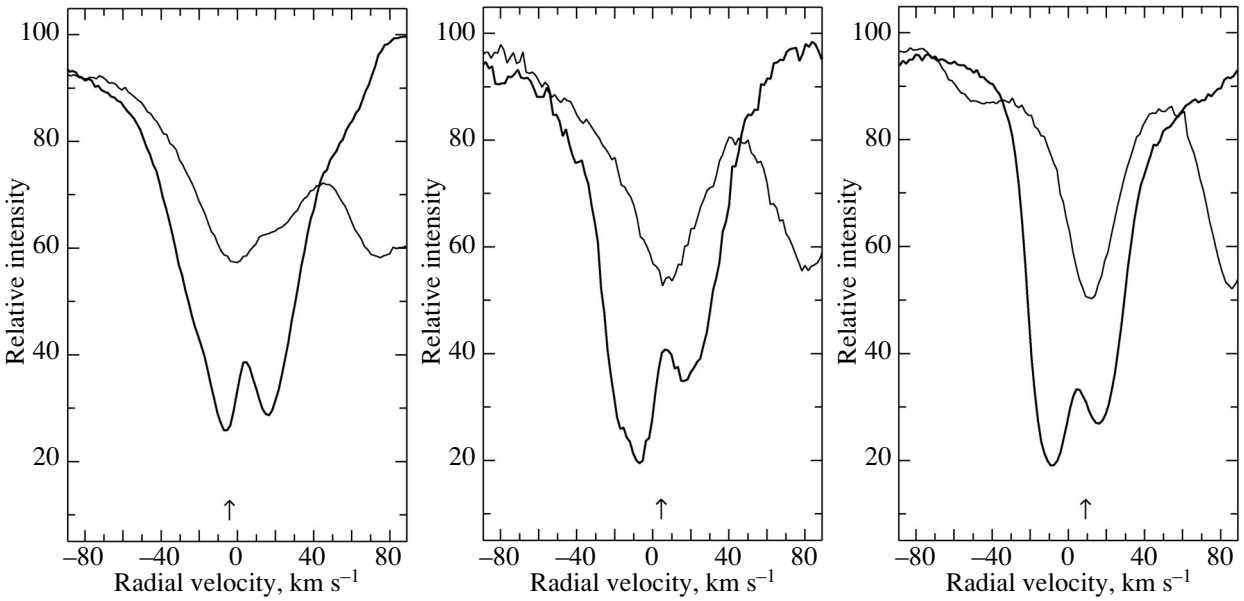

Fig. 4. Fe II 6147 Å (thin curve) and Ba II 6141 Å (thick solid curve) line profiles in the October 13, 2013, April 28, 2015, and September 3, 2015 spectra of V1027 Cyg. The arrows indicate the mean radial velocities V_r(abs.) from Table 2 measured from symmetric absorptions in the spectra for each time of observations.

various types of spectral features in the available spectra of V1027 Cyg. We will rely on these data in our subsequent analysis of the spectrum peculiarities.

The mean velocities V_r(abs.) corresponding to the positions of extensive samples of symmetric absorptions are given in column 4 of Table 1. For three dates of observations we obtained radial velocities in the range from -4.1 ± 0.1 to $+9.1 \pm 0.1$ km s^{-1}. This variability of V_r(abs.) is a manifestation of the pulsations of the V1027 Cyg atmosphere. Recall that the temperature of V1027 Cyg is $T_{\rm eff} = 5000$ K, which, according to Soker (2008), is close to the boundary of the transition from the AGB stage to the succeeding post AGB one. As follows from the paper by Aikawa (2010), the AGB star with parameters $T_{\rm eff} = 5000$ K and $\log g = 1.0$ entered the instability strip and can have radial pulsations. Having analyzed the long-term behavior of the UBV data for V1027 Cyg, Arkhipova et al. (2000) reached the conclusion about pulsations of the star in the fundamental mode and the first overtone with periods of $P \approx 306$ and 250 days.

The results of our radial velocity measurements from the position of the component in the strongest absorptions are quite unexpected. The mean velocities from the full profiles of these strong features V_r(full) are given in the last column of Table 2. The accuracy of measuring the position of the full profile for the split absorptions is lower than that for the remaining features of their profile due to its asymmetry. However, the accuracy is sufficient to conclude that the positions of the profiles are constant. These positions of the strong absorptions are clearly seen in Fig. 4, where the profiles of the strong Ba II 6141 Å line and the moderate-intensity Fe II 6147 Å line for three times of observations are compared on separate panels. Here, the position of the weak Fe II 6147 Å line in each spectrum coincides with the mean radial velocity inferred from symmetric absorptions V_r(abs.). At the same time, the position of the full Ba II 6141 Å profile barely changes from date to date and does not correspond to V_r(abs.). This behavior can be explained by the formation of this line in the outer atmospheric layers unaffected by pulsations.

For the strong absorptions we additionally measured the positions of the short-wavelength, V_r(blue), and long-wavelength, V_r(red), components as well as the position of the emission peak between them V_r(emis). The results of our V_r measurements from these components and their errors are given in Table 2, columns 2–4, whence we conclude that the radial velocities in columns 2–4 measured with a high accuracy are constant with time. It follows from the constant positions of the emission features that they are formed in the envelope regions that are external with respect to the supergiant's photosphere.

We have already noted above that the neutral hydrogen line profile is an absorption without any clear peculiarities expected for a G-type supergiant. However, as follows from Table 1, the position of the Hα core systematically differs from the expected one corresponding to the mean radial velocity V_r(abs.) for the corresponding date. A possible explanation of the Hα position in the spectrum is suggested by Fig. 1, where an asymmetry of the line core apparently attributable to the influence of an aspherical

Table 2. Mean heliocentric radial velocities V_r measured from the features of strong absorptions: from the cores of the short-wavelength, V_r(blue), and long-wavelength, V_r(red), components, from the emission peak V_r(emis), and from the full profile V_r(full). The number of measured features is given in parentheses

Date	V_r, km s^{-1}			
	blue	emis	red	full
Oct. 13, 2013	-5.2 ± 0.2 (63)	4.6 ± 0.1 (82)	16.0 ± 0.1 (83)	6.2 ± 0.3 (26)
Apr. 28, 2015	-5.0 ± 0.3 (28)	6.1 ± 0.1 (15)	15.5 ± 0.2 (17)	3.3 ± 0.5 (7)
Sep. 3, 2015	-5.1 ± 0.3 (28)	5.4 ± 0.2 (33)	16.4 ± 0.2 (29)	4.7 ± 0.3 (27)

envelope is clearly seen for all three times of observations. Evidence for asphericity of the V1027 Cyg envelope also follows from the high degree of polarization ($P = 7.7\%$) that was determined by Trammell et al. (1994) from spectropolarimetric observations. Subsequently, having performed multicolor polarimetric photometry, Parthasarathy et al. (2006) obtained a degree of polarization $\sim$1%.

In the far red region of the spectrum for V1027 Cyg we identified CN molecular lines. A fragment of the spectrum in the region 7960–8000 Å containing many weak lines (with depths 10–15% below the continuum level) is presented in Fig. 6. We took the wavelengths for the CN features from the VALD database. The coincidence of the radial velocities measured from symmetric metal absorptions and CN lines points to the formation of the CN spectrum in the atmosphere of V1027 Cyg, which is natural for such a cool star.

Interstellar Features and the Systemic Velocity Problem

Apart from the numerous absorptions forming in the supergiant's atmosphere, we detected at least ten weak absorptions in each spectrum of V1027 Cyg whose positions allowed them to be identified with DIBs. Table 1 gives the mean velocities corresponding to the positions of these features. Given the results of Vallee (2008), the velocity averaged over three spectra, $V_r(\mathrm{DIBs}) = -12.0$ km s^{-1}, corresponds to the velocity of the interstellar medium in the Local Arm of the Galaxy.

Consider in more detail Fig. 5, where the Na I and K I 7696 Å line profiles are compared and the mean velocities inferred from numerous symmetric absorptions, $V_r(\mathrm{abs.}) = 4.5$ km s^{-1}, and DIBs, $V_r(\mathrm{DIB}) = -12.9$ km s^{-1}, for a given date of observations are indicated. Here, it can be seen that apart from the photospheric and interstellar ($V_r(\mathrm{IS}) = -12.0$ km s^{-1}) components, the broad Na I D line profile apparently contains the circumstellar and additional interstellar components ($V_r \leq -17.0$) that are not separated at the spectral resolution of the NES spectrograph. The interstellar components of these lines merge together to form a broad absorption in the velocity range from $V_r \approx -17.0$ to -33.0 km s^{-1}. The longest-wavelength component with $V_r \approx -12.0$ km s^{-1}, just as the DIBs, is formed in the Local Arm of the Galaxy (Vallee 2006). As follows from Fig. 5 and the data in the last column of Table 1, the position of the absorption component of the K I 7696 Å line with $V_r \approx -12$ km s^{-1} is consistent with the DIB positions. This coincidence may point to an interstellar formation of the K I absorption component.

The presence of a short-wavelength component with $V_r \approx -33.0$ km s^{-1}, which, according to Vallee (2006), corresponds to the velocities in the Perseus arm, points to a more distant position of the star. We emphasize that Kipper and Klochkova (2006) revealed the same interstellar velocity components ($V_r \approx -12.0$ and -33.0 km s^{-1}) in the spectrum of the faint star that is the optical counterpart of the IR source IRAS 20000+3239 with Galactic coordinates close to those of V1027 Cyg: l/b $\approx$ 69/01 and 67/00 for IRAS 20000+3239 and V1027 Cyg, respectively.

The absence of information about the star's systemic velocity prevents us from unambiguously interpreting the pattern of radial velocities in the atmosphere and envelope of V1027 Cyg. There is no information about the detection of molecular or maser emission in the published data on radio spectroscopy for IRAS 20004+2955 (Eder et al. 1987; Lewis et al 1987; Bujarrabal et al. 1992). In the absence of such data, as the systemic velocity of V1027 Cyg we may take $V_{\mathrm{sys}} \approx 5.5$ km s^{-1}, which is the value of V_r averaged over all the emissions we detected: in the cores of the strong metal lines from Table 2 and $V_e(7696) = 6.1$ km s^{-1} from the emission in the K I 7696 Å line.

All of the available V_r measurements based on the atmospheric absorptions from Table 2 with those published previously by Klochkova et al. (2000a) fall within the narrow range -4.1–10.3 km s^{-1}. The adopted systemic velocity $V_{\mathrm{sys}} = 5.5$ km s^{-1} leads to

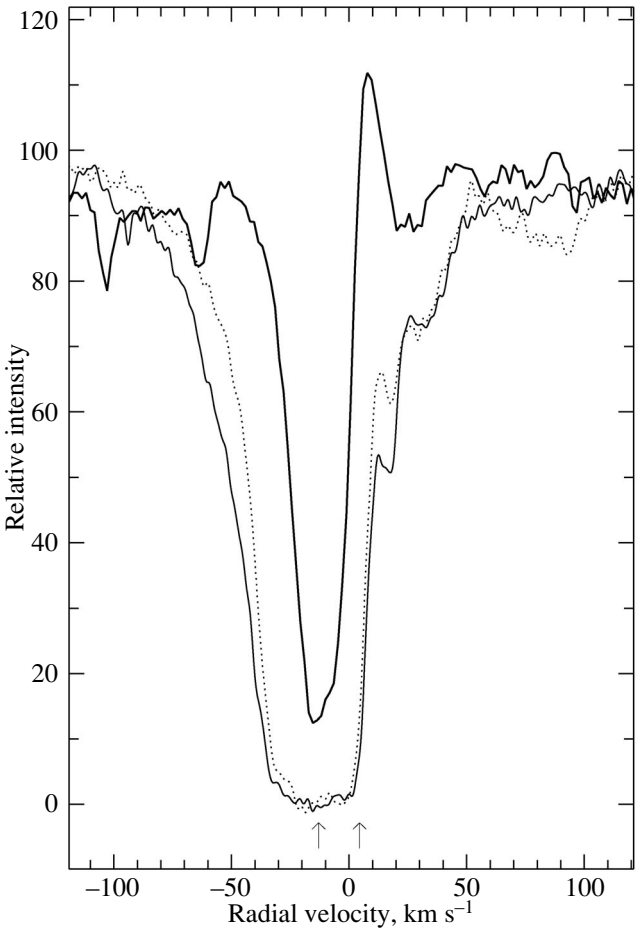

Fig. 5. Na I 5889 Å (thin curve), 5895 Å (dotted curve), and K I 7696 Å (thick solid curve) line profiles in the April 28, 2015 spectrum of V1027 Cyg. The arrows indicate the velocities in the spectrum for this date from Table 2 estimated from symmetric photospheric absorptions and DIBs: V_r(abs.) = 4.5 km s^{-1} and V_r(DIB) = −12.9 km s^{-1}, respectively.

the tentative conclusion about a small radial velocity amplitude attributable to pulsations. Recall that Arkhipova et al. (1997) obtained a wider range of values, $V_r = -10 - +20$ km s^{-1}, from low-resolution spectra.

DISCUSSION

Anomalous profiles of strong absorptions (Si II, Ni I, Ti I, Ti II, Sc II, Cr I, Fe I, Fe II, Ba II) have been detected in the spectrum of V1027 Cyg for the first time. Our measurements of the positions of individual features in these absorptions allow the profiles of these lines to be considered as a single broad absorption whose position does not correspond to V_r(abs.) and does not change from date to date. This discrepancy between the velocities inferred from strong and weak absorptions can be explained by the fact that the strong absorptions are formed in the outer layers of the extended atmosphere unaffected by pulsations. Stable weak emissions are observed in the cores of all the strongest absorptions. The mean velocity of these emissions, in the absence of radio spectroscopic data for the IR source IRAS 20004+2955, may be considered as the systemic velocity V_{sys} = 5.5 km s^{-1}. Similar peculiarities of the spectrum are observed in R Sct, an RV Tau variable star, whose evolutionary status is close to the evolutionary stage of V1027 Cyg. For example, Kipper and Klochkova (2013) pointed out a splitting of the strongest absorptions in the spectrum of R Sct and the presence of a weak and variable emission in Fe I and Ti I lines. However, as has been noted above, in contrast to V1027 Cyg, the spectrum of R Sct near minimum light exhibits an emission in Hα and Hβ as well.

Line doubling is a fairly common phenomenon observed in the spectra of variable stars of various types. The propagation of a shock wave is a universally accepted cause of the double absorption lines in the spectra of pulsating stars (for the details of this Schwarzschild scenario, see Alvarez et al. (2000). The line doubling in the spectra for an extensive sample of Mira variables was investigated by Alvarez et al. (2001). One of the most important results of their publication is that there is no visual-amplitude threshold beyond which line doubling only would occur in small-amplitude stars.

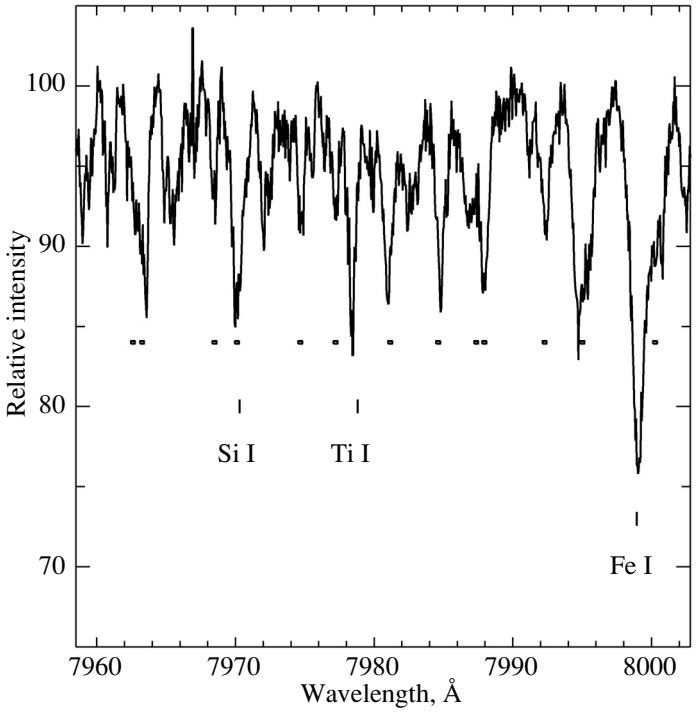

Fig. 6. Fragment of the spectrum for V1027 Cyg. The dots mark the CN lines. The identified strongest (within this fragment) metal absorptions are also indicated.

Recall that doubling or asymmetry of strong absorptions were detected in the spectra of a small group of selected post-AGB stars. In contrast to V1027 Cyg, the atmospheres of all stars from this sample are enriched with carbon and heavy metals. In particular, through a spectroscopic monitoring with a high spectral resolution Klochkova (2013) detected a splitting of strong absorptions with a low lower-level excitation potential in the spectrum of the post-AGB supergiant V5112 Sgr for the first time. Invoking the radio spectroscopic data for the associated IR source IRAS 19500−1709 led to the conclusion that the short-wavelength components of the split absorptions are formed in a structured circumstellar envelope. Thus, evidence for an efficient dredge-up of the heavy metals produced during the preceding evolution of this star into the envelope was obtained. A similar effect was detected (Klochkova et al. 2015) in the spectrum of the optically faint star associated with the IR source IRAS 23304+6147, with large overabundances of carbon and heavy metals having been revealed in its atmosphere (Klochkova et al. 2000b). The general properties of a sample of post-AGB supergiants with a splitting of strong absorptions are summarized in Klochkova and Panchuk (2016), where it was shown that the type of profiles for strong absorptions could be connected with the morphology of the envelope and with its kinematic and chemical properties.

However, despite the fact that the anomalies of the profiles of strong absorptions in the spectra of the mentioned post-AGB stars and V1027 Cyg are similar in appearance, we reached the tentative conclusion that the causes of the profile distortion in the spectra of these objects are different. In the spectra of post-AGB stars at least one of the components of the split absorptions is formed in the envelope detached from the central star. In contrast, in the case of V1027 Cyg, the strong absorptions with split cores are formed in the upper layers of the extended stellar atmosphere. Their positions are, on the whole, stable; the pulsations manifest themselves as a weak variability of the short-wavelength wings. Thus, the kinematics in the atmosphere of V1027 Cyg can be said to be stratified: small-amplitude pulsations are observed in deep layers of the stellar atmosphere, while the upper atmospheric layers are stable. Using their IR observations with the VLT, Lagadec et al. (2011) studied the images for a large sample of supergiants and showed the image of V1027 Cyg to be point-like; the circumstellar dust envelope is not resolved.

The DIB positions, $V_r(\mathrm{DIBs}) = -12.0$ km s^{-1}, correspond to the velocity of the interstellar medium in the Local Arm of the Galaxy (Y.P. Georgelin and Y.M. Georgelin 1970). Using the adopted systemic velocity $V_{\mathrm{sys}} \approx 5.5$ km s^{-1} (LSR ≈ 23 km s^{-1}) and the data from Brand and Blitz (1993) on the velocity field in the Galaxy, we can estimate the distance to the star, $d = 3.9$ kpc. This estimate agrees well with the distance to V1027 Cyg that Bogdanov and Taranova (2009) obtained by an independent method.

The IR spectrum of V1027 Cyg = IRAS 20004+2955 exhibits a strong emission at 10 μm identified with silicates in the stellar envelope. This emission, which is typical of the spectra of O-rich stars, served to Hrivnak et al. (1989) as a basis to consider IRAS 20004+2955 to be an analog of the well-studied source IRAS 18095+2704. However, the central stars of these IR sources differ in metallicity. For IRAS 18095+2704 [Fe/H] = from -0.8 to -0.9, according to Klochkova (1995) and Sahin et al. (2011), respectively, while in the atmosphere of V1027 Cyg, as Klochkova et al. (2000a) showed, the metallicity is nearly solar: [Fe/H] = -0.2. The high metallicity of V1027 Cyg and its location close to the Galactic plane suggest that this star belongs to the disk population.

We think the central star of the IR source IRAS 20508+2011 already mentioned in the text to be a closer relative for V1027 Cyg. The parameters of this star derived by Klochkova et al. (2006) (its luminosity $M_v \approx -3^m$, effective temperature $T_{\rm eff} = 4800$ K, surface gravity $\log g = 1.5$, metallicity $\mathrm{Fe/H}_\odot = -0.36$, and chemical composition) are typical of an AGB star. The ratio of the carbon and oxygen overabundances allows IRAS 20508+2011 to be assigned to the group of evolved stars with oxygen-enriched atmospheres ([O/C] = $+0.9$), which is consistent with the object's position on the IR color–color diagram. No overabundance of s-process elements was detected, just as in V1027 Cyg. Since as yet there are no observations in water maser and OH bands for IRAS 20508+2011, we cannot unambiguously classify the envelope. However, it can be asserted that in the case of IRAS 20508+2011 we observe an extremely early PPN formation phase that comes immediately after the termination of mass loss and apparently until the beginning of envelope separation.

As has already been noted by Klochkova et al. (2000a), the set of main parameters of V1027 Cyg (the location of this star close to the Galactic plane, its nearly solar metallicity, and the atmospheric abundances of chemical elements) more likely corresponds to a classical supergiant, especially since the intensity of the O I λ7771–7775 Å triplet, which served as a universally accepted luminosity indicator, is very high in the spectrum of this star. The total equivalent width of the triplet in the spectrum of V1027 Cyg is W(7773) = 1.86 Å. Applying the Mv–W(7773) calibrations published by Klochkova et al. (2002) and Arellano Ferro et al. (2003), we obtain the luminosity $M_v = -8.0^m$ for V1027 Cyg, which is considerably higher than the luminosity of AGB stars but agrees well with luminosity class Ia. However, we should keep in mind the possible error in the luminosity due to the application of the M_v–$W(7773)$ calibration obtained from Cepheids and other massive A–G supergiants of the Galactic disk to a star with an unclear evolutionary status and the neglect of possible differences in oxygen abundance.

Taking the luminosity of the star to be $M_v = -8.0^m$ and the color excess to be $E(B-V) = 0.6^m$ (Arkhipova et al. 2000), we estimate the distance to V1027 Cyg to be $d \approx 7.5$ kpc, which exceeds considerably the distance $d = 3.9$ kpc corresponding to the systemic velocity of the star we adopted. The unreliability of the color excess and systemic velocity estimates is responsible for the discrepancy. For example, if we use the interstellar reddening $A_v = 3.6^m$ estimated by Hrivnak et al. (1989) for V1027 Cyg by modeling the flux in the wide wavelength range 0.4–100 μm, then we will obtain $d \approx 4.0$ kpc. This value agrees well with the distance inferred from the systemic velocity.

To refine our conclusions about the star V1027 Cyg, we need its spectroscopic monitoring with an ultrahigh spectral resolution ($R \geq 10^5$) that will ensure the separation of the components of the Na I D and K I 7696 Å line profiles, the refinement of the proposed velocity pattern, and, consequently, the refinement of the distance to the star and its evolutionary status.

CONCLUSIONS

Based on our high-spectral-resolution observations performed with the NES echelle spectrograph of the 6-m telescope, we detected the peculiarities of the spectrum and the velocity field in the atmosphere of the cool supergiant V1027 Cyg, the optical counterpart of the IR source IRAS 20004+2955. Small variations of the radial velocity V_r(abs.) with an amplitude of about 5 km s^{-1} due to pulsations were revealed by symmetric low- and moderate-intensity absorptions.

Numerous weak CN molecular lines and the KI 7696 Å line with a P Cyg profile were identified in the red spectral region. The coincidence of the radial velocities measured from symmetric metal absorptions and CN lines suggests that the CN spectrum is formed in the stellar atmosphere. We identified numerous diffuse interstellar bands (DIBs) whose positions in the spectrum, V_r(DIBs) = -12.0 km s^{-1}, correspond to the velocity of the interstellar medium in the Local Arm of the Galaxy.

A long-wavelength and time-variable shift of the Hα profile due to line core and short-wavelength wing distortion is observed in the spectrum of V1027 Cyg. A splitting of the cores of the strongest absorptions of metals and their ions (Si II, Ni I, Ti I, Ti II, Sc II, Cr I,

Fe I, Fe II, Ba II) has been detected in the stellar spectrum for the first time. The broad profile of these lines contains a stable weak emission in the core whose position may be considered as the systematic velocity $V_{sys} = 5.5$ km s^{-1}. Spectroscopy with an ultrahigh spectral resolution is needed for a more definite interpretation of the radial velocity pattern, for identifying the circumstellar and photospheric components in the Na I D line profile, and, consequently, for refining the distance to the star and its evolutionary status.

ACKNOWLEDGMENTS

This work was supported by the Russian Foundation for Basic Research (project nos. 14-02-00291a and 16-02-00587a). We used the SIMBAD and ADS astronomical databases. We also used the VALD database maintained in the Uppsala and Vienna Universities and at the Institute of Astronomy of the Russian Academy of Sciences (Moscow).

REFERENCES

1. T. Aikawa, Astron. Astrophys. **514**, A45 (2010).
2. R. Alvarez, A. Jorissen, B. Plez, D. Gillet, and A. Fokin, Astron. Astrophys. **362**, 655 (2000).
3. R. Alvarez, A. Jorissen, B. Plez, D. Gillet, A. Fokin, and M. Dedecker, Astron. Astrophys. **379**, 305 (2001).
4. A. Arellano Ferro, S. Giridhar, and E. Rojo Arellano, Rev. Mex. Astron. Astrofis. **39**, 3 (2003).
5. V. P. Arkhipova, N. P. Ikonnikova, R. I. Noskova, and S. Yu. Shugarov, Astron. Lett. **18**, 175 (1992).
6. V. P. Arkhipova, V. F. Esipov, N. P. Ikonnikova, R. I. Noskova, S. Yu. Shugarov, and N. A. Gorynya, Astron. Lett. **23**, 690 (1997).
7. V. P. Arkhipova, V. F. Esipov, N. P. Ikonnikova, R. I. Noskova, and G. V. Sokol, Astron. Lett. **26**, 609 (2000).
8. M. B. Bogdanov and O. G. Taranova, Astron. Rep. **53**, 850 (2009).
9. J. Brand and I. Blitz, Astron. Astrophys. **275**, 67 (1993).
10. V. Bujarrabal, J. Alcolea, and P. Planesas, Astron. Astrophys. **257**, 701 (1992).
11. J. Eder, B. M. Lewis, and Y. Terzian, Publ. Astron. Soc. Pacif. **99**, 1147 (1987).
12. G. A. Galazutdinov, Preprint SAO RAN No. 92 (Spec. Astrophys. Observ., Zelenchuk, 1992).
13. Y. P. Georgelin and Y. M. Georgelin, Astron. Astrophys. **6**, 349 (1970).
14. B. J. Hrivnak and L. Wenxian, in *Carbon Star Phenomenon, Proceedings of the 177th Symposium of the International Astronomical Union, Antalya, Turkey, May 27–31, 1996,* Ed. R. F. Wing (Kluwer Academic, Dordrecht, 2000), p. 293.
15. B. J. Hrivnak, S. Kwok, and K. Volk, Astrophys. J. **346**, 265 (1989).
16. P. C. Keenan and R. C. McNeil, Astrophys. J. Suppl. Ser. **71**, 245 (1989).
17. T. Kipper and V. G. Klochkova, Baltic Astron. **15**, 395 (2006).
18. T. Kipper and V. G. Klochkova, Baltic Astron. **22**, 77 (2013).
19. V. G. Klochkova, Mon. Not. R. Astron. Soc. **272**, 710 (1995).
20. V. G. Klochkova, Astron. Lett. **39**, 765 (2013).
21. V. G. Klochkova, Astrophys. Bull. **69**, 279 (2014).
22. V. G. Klochkova and V. E. Panchuk, Astron. Rep. **60**, 344 (2016).
23. V. G. Klochkova, T. V. Mishenina, and V. E. Panchuk, Astron. Lett. **26**, 398 (2000a).
24. V. G. Klochkova, R. Szczerba, and V. E. Panchuk, Astron. Lett. **26**, 88 (2000b).
25. V. G. Klochkova, M. V. Yushkin, E. L. Chentsov, and V. E. Panchuk, Astron. Rep. **46**, 139 (2002).
26. V. G. Klochkova, V. E. Panchuk, N. S. Tavolganskaya, and G. Zhao, Astron. Rep. **50**, 232 (2006).
27. V. G. Klochkova, V. E. Panchuk, and N. S. Tavolganskaya, Astron. Lett. **41**, 14 (2015).
28. S. Kwok, Ann. Rev. Astron. Astrophys. **31**, 63 (1993).
29. E. Lagadec, T. Verhoelst, D. Mekarnia, O. Suárez, A. A. Zijlstra, P. Bendjoya, R. Szczerba, et al., Mon. Not. R. Astron. Soc. **417**, 32 (2011).
30. A. Lèbre and D. Gillet, Astron. Astrophys. **246**, 490 (1991).
31. B. M. Lewis, J. Eder, and Y. Terzian, Astrophys. J. **94**, 1025 (1987).
32. V. E. Panchuk, J. D. Najdenov, V. G. Klochkova, A. V. Ivanchik, S. V. Yermakov, and V. A. Murzin, Bull. Spec. Astrophys. Observ. **44**, 127 (1997).
33. V. E. Panchuk, M. V. Yushkin, and I. D. Naidenov, Preprint SAO RAN No. 179 (Spec. Astrophys. Observ., Zelenchuk, 2003).
34. V. E. Panchuk, V. G. Klochkova, M. V. Yushkin, and I. D. Naidenov, J. Opt. Technol. **76**, 87 (2009).
35. M. Parthasarathy, S. K. Jain, and G. Sarkar, Astron. J. **129**, 2451 (2006).
36. T. Sahin, D. L. Lambert, V. G. Klochkova, and N. S. Tavolganskaya, Mon. Not. R. Astron. Soc. **410**, 612 (2011).
37. N. Soker, Astrophys. J. **674**, L49 (2008).
38. O. G. Taranova, V. I. Shenavrin, and A. M. Tatarnikov, Astron. Lett. **35**, 472 (2009).
39. S. R. Trammell, H. L. Dinerstein, and R. W. Goodrich, Astron. J. **108**, 984 (1994).
40. J. P. Vallee, Astron. J. **135**, 1301 (2006).
41. K. M. Volk and S. Kwok, Astrophys. J. **342**, 345 (1989).
42. M. V. Yushkin and V. G. Klochkova, Preprint SAO RAN No. 206 (Spec. Astrophys. Observ., Zelenchuk, 2005).

Translated by V. Astakhov